Journal of Colloid and Interface Science 405 (2013) 51–57

Contents lists available at SciVerse ScienceDirect

Journal of Colloid and Interface Science

www.elsevier.com/locate/jcis

Self-assembled biomimetic superhydrophobic hierarchical arrays

Hongta Yang [a,*], Xuan Dou [b], Yin Fang [b], Peng Jiang [b,*]

[a] Department of Chemical Engineering, National Chung Hsing University, 250 Kuo Kuang Road, Taichung, Taiwan
[b] Department of Chemical Engineering, University of Florida, Gainesville, FL 32611, USA

ARTICLE INFO

Article history:
Received 22 February 2013
Accepted 16 May 2013
Available online 24 May 2013

Keywords:
Superhydrophobic
Self-assembly
Hierarchical arrays
Biomimetic
Templating

ABSTRACT

Here, we report a simple and inexpensive bottom-up technology for fabricating superhydrophobic coatings with hierarchical micro-/nano-structures, which are inspired by the binary periodic structure found on the superhydrophobic compound eyes of some insects (e.g., mosquitoes and moths). Binary colloidal arrays consisting of exemplary large (4 and 30 μm) and small (300 nm) silica spheres are first assembled by a scalable Langmuir–Blodgett (LB) technology in a layer-by-layer manner. After surface modification with fluorosilanes, the self-assembled hierarchical particle arrays become superhydrophobic with an apparent water contact angle (CA) larger than 150°. The throughput of the resulting superhydrophobic coatings with hierarchical structures can be significantly improved by templating the binary periodic structures of the LB-assembled colloidal arrays into UV-curable fluoropolymers by a soft lithography approach. Superhydrophobic perfluoroether acrylate hierarchical arrays with large CAs and small CA hysteresis can be faithfully replicated onto various substrates. Both experiments and theoretical calculations based on the Cassie's dewetting model demonstrate the importance of the hierarchical structure in achieving the final superhydrophobic surface states.

1. Introduction

Nature is the ultimate nanotechnologist. Through millions of years of evolution, biological systems have developed and adapted a wide spectrum of unique architectures for advanced functionalities, such as antireflective moth eyes [1,2], self-cleaning lotus leaves [3–8], water-capturing beetles and spiders [9,10], diffractive Morpho butterfly wings [11–13], adhesive gecko feet [14,15], ultrastrong nacres [16,17], and many more [18,19]. Hierarchically arranged micro-/nano-structures are also abundant in the biological world, and almost all above-mentioned biological functions require some sort of hierarchical structures for them to work [2,4,18,19]. One prominent example is the compound eyes of some insects, such as mosquitoes, butterflies, and moths. The outer surfaces of the hexagonally close-packed, hemispherically shaped corneal lenses (termed ommatidia) with typical diameters ranging from a few micrometers to ~30 μm for different species are covered with periodic hexagonal arrays of nanoscale corneal nipples with typical height and spacing of sub-300 nm [1,2,20]. In addition to rendering broadband antireflection which has been extensively exploited [1,21–24], this hierarchical micro-/nano-structure also enables efficient trapping of a large fraction of air in between ommatidia, resulting in superhydrophobic coatings with large water CAs [20].

To mimic the hierarchically structured compound eyes for making superhydrophobic coatings, a large variety of top-down and bottom-up technologies have been developed [20,23,25–35]. Among these different approaches, colloidal self-assembly is perhaps the most versatile methodology in creating highly ordered hierarchical structures [36–42] as many mature self-assembly techniques [43–45] and highly uniform colloidal particles with a wide range of sizes are readily available. For instance, Gao et al. combined photolithography with soft lithography to fabricate binary arrays of silica nanoparticles on large periodic polydimethylsiloxane (PDMS) hemispheres [20]. Superhydrophobic hierarchical structures made by combining colloidal self-assembly with annealing-induced dewetting of sputtered gold films have also been demonstrated [34]. Random deposition of raspberry-like particles consisting of large and small spheres is another approach in assembling hierarchical superhydrophobic films [31,32]. Replica molding [30] and nanoimprinting [23] have been employed in making large periodic microstructures which can be covered with colloidal nanoparticles in the subsequent steps. Dip coating and spin coating are also widely used in assembling binary particle arrays [33,46]. However, many of these techniques either require a lithographic step in making the microstructures [20,23], or the resulting particle arrays are randomly arranged [31–33,46], or the sizes of the final micro- and/or nano-structures do not match with those of natural compound eyes. All these drawbacks could

* Corresponding authors. Fax: +1 352 392 9513 (P. Jiang), +886 4 2285 4734 (H. Yang).
E-mail addresses: hyang@dragon.nchu.edu.tw (H. Yang), pjiang@che.ufl.edu (P. Jiang).

0021-9797/$ - see front matter © 2013 Elsevier Inc. All rights reserved.
http://dx.doi.org/10.1016/j.jcis.2013.05.040

affect the cost effectiveness and the uniformity/reproducibility of the structured superhydrophobic substrates.

Here, we report a simple bottom-up technology for fabricating superhydrophobic hierarchical arrays with the periodic structure and size mimicking those of natural corneal lenses. Binary close-packed colloidal arrays consisting of exemplary large (4 and 30 μm) and small (300 nm) silica particles are going to be deposited by the LB technique, which has recently been demonstrated in assembling wafer-scale colloidal monolayers as efficient antireflection coatings [47,48]. Templating fabrication of monolithic fluoropolymer hierarchical arrays that exhibit large water CAs and small CA hysteresis will also be demonstrated. In addition, experimental CA measurements will be complemented by theoretical calculation based on the Cassie's model [49] to gain better understanding of the dewetting properties of the self-assembled and templated superhydrophobic hierarchical arrays.

2. Experimental

2.1. Materials and substrates

All solvents and chemicals are of reagent quality and are used without further purification. Large silica spheres with 4 and 30 μm diameters and less than 10% diameter standard deviation are purchased from Particle Solutions LLC (Alachua, Florida). Monodispersed silica microspheres with 300 nm diameter are synthesized by the standard Stöber process [50]. The reagents used for the synthesis of silica microspheres including tetraethyl orthosilicate (TEOS, 98%) and ammonium hydroxide (28%) are purchased from Sigma–Aldrich. Ethanol (200-proof) is obtained from Decon Labs. (tridecafluoro-1,1,2,2,-tetrahydrooctyl)-trichlorosilane (97%) used for surface modification and ethylene glycol (99%) are obtained from Alfa Aesar. Two-part PDMS precursors (Sylgard 184) are provided by Dow Corning. De-ionized water (18.2 MΩ cm) is used directly from a Millipore A-10 water purification system. The UV-curable perfluoroether acrylate monomer (UV-T) is synthesized by following the established procedures using commercial perfluorinated alkylene diols (Exfluor) as starting materials [51,52]. The photoinitiator, Darocur 1173 (2-hydroxy-2-methyl-1-phenyl-1-propanone), is provided by BASF Corporation. Silicon wafers (test grade, n type, (100), Wafernet) and glass microslides (Fisher) are cleaned in a "Piranha" solution (a 3:1 mixture of concentrated sulfuric acid with 30% hydrogen peroxide) for half an hour, rinsed with de-ionized water, and dried in a stream of nitrogen.

2.2. Instrumentation

A KD Scientific 780-230 syringe pump is used to precisely control the withdrawal speed of the substrate in the LB colloidal assembly process. Scanning electron microscopy (SEM) is carried out on a JEOL 6335F FEG-SEM. A thin layer of gold is sputtered onto the samples prior to imaging. Fourier Transformed Infrared Spectroscopy (FTIR) of UV-T is performed using a Thermo Electron Magna 760 spectrometer. A pulsed UV curing system RC 742 (Xenon) is used to cure UV-T monomers. Water CAs on different surfaces are measured by using a dynamic CA analyzer (Ramé-Hart Goniometer) at ambient temperature with a droplet volume of 7.5 μL.

2.3. LB assembly of binary colloidal arrays

The as-synthesized small silica microspheres (300 nm) are first purified by multiple (at least 5 times) centrifugation/redispersion cycles in ethanol and then redispersed in ethylene glycol. The large silica spheres (4 and 30 μm, provided as dry powders) are directly dispersed in ethylene glycol. The particle volume fractions for both small and large sphere suspensions are controlled to be 0.20. Using a clamp attached to the syringe pump, the cleaned substrate is vertically immersed in a Kimax crystallizing dish (170 × 90 mm) containing de-ionized water. The silica/ethylene glycol suspension is added dropwise to the water surface. The silica spheres rapidly spread to form a colloidal monolayer, floating at the air/water interface. For small silica particles, the floating layers exhibit iridescent colors caused by Bragg diffraction of visible light from the colloidal arrays [53]. The crystalline quality of the large sphere arrays can be improved by gently tapping the sidewall of the crystallizing dish to facilitate the merging of small crystal domains into larger ones. The substrate is then withdrawn at a rate of ~12.5 mm/min controlled by the syringe pump. As the substrate is withdrawn, the floating colloidal monolayers are transferred onto both sides of the substrate. In this work, we first assemble large silica spheres (4 and 30 μm) on the substrate using the LB method. After drying in air, the substrate is re-immersed in water, and a colloidal monolayer of 300 nm silica microspheres is subsequently deposited on the surfaces of the large spheres.

2.4. Surface modification of binary colloidal arrays

The hydrophobicity of the LB-assembled binary colloidal arrays can be improved by surface modification using fluorosilanes through the well-established silane coupling reactions [54,55]. The sample is placed in a vacuum oven with a beaker containing a small amount (~20 mL) of (tridecafluoro-1,1,2,2,-tetrahydrooctyl)-trichlorosilane. The oven is then heated up to 120 °C to enable the hydrolyzed silane groups of the fluorosilane vapor to react with the hydroxyl groups on the silica spheres. After 1 h, the sample is removed from the oven and heated at 150 °C for 1 h on a digital hot plate in air to vaporize the unreacted fluorosilane adsorbed on the sample.

2.5. Templating fabrication of hierarchical fluoropolymer arrays

The hierarchical micro-/nano-structure of the LB-assembled binary colloidal arrays can be easily transferred to a PDMS mold by pouring mixed and degassed PDMS precursors onto the sample and then heated at 70 °C for 30 min. The solidified PDMS mold is peeled off and then put on top of a small amount of UV-T monomers supported by a silicon wafer or a glass microslide with spacers (double-stick tape, thickness ~0.1 mm) in between. The UV-T monomers are photopolymerized for 2 s using the Xenon pulsed UV curing system. After peeling off the PDMS mold, fluoropolymer arrays with hierarchical structures are resulted.

2.6. Water contact angle measurements

All samples are first blown with filtered air to remove contaminants on their surface. The apparent water CA is then measured using a Ramé-Hart Goniometer with autopipetting and imaging systems. De-ionized water from the Millipore Water System is used for the contact angle measurement. A micropipette tip attached to the autopipetting system is lowered to approximately 1 mm above the sample surface. Using the autopipetting system and DROP image advanced software, a 7.5 μL water drop is dispensed onto the sample surface. The pipette tip is then raised, and an image of the drop is taken. This process is repeated 8 times for each sample. The drop is placed on a different region of the sample for each image. Apparent water CA is determined from the images using ImageJ v1.37 with the drop analysis plugin. Analysis of each image yields a left and right contact angle for each drop, yielding 16 angle measurements per sample. The average of these 16 values is the apparent water CA reported.

3. Results and discussion

The schematic illustration for sequentially assembling binary colloidal arrays consisting of large and small silica spheres and templating the assembled arrays in fluoropolymer is shown in Fig. 1. Monolayers of large silica spheres (4 and 30 μm) floating at the air/water interface are first transferred onto the surface of the substrate (e.g., silicon wafer or glass microslide) using the LB assembly technology [47,48]. After drying in air, the substrate is re-immersed in water, and monolayers of small (300 nm) silica microspheres assembled at the air/water interface are subsequently deposited on the contoured surfaces of the close-packed large spheres. Importantly, no post-treatment (e.g., thermal annealing) of the large sphere array is needed prior to the LB assembly of the small silica microspheres. The as-assembled binary colloidal arrays can be directly used as superhydrophobic substrates after a simple surface modification process using (tridecafluoro-1,1,2,2,-tetrahydrooctyl)-trichlorosilane as the silane coupling agent [54,55]. Otherwise, the hierarchical micro-/nanostructure of the binary colloidal array can be templated into a PDMS mold, and a soft molding process is finally employed to replicate the hierarchical structure into UV-curable perfluoroether acrylates (e.g., UV-T).

Fig. 2A shows a photograph of a glass microslide (75 × 25 mm) partially covered with a LB-assembled monolayer of 4 μm silica spheres. Indeed, both sides of the glass substrate are coated with uniform monolayers of the large silica spheres. The typical optical microscope image in Fig. 2B and the hexagonally arranged sharp peaks in the Fourier transform of a lower-magnification optical microscope image (inset of Fig. 2B) illustrate the high crystalline

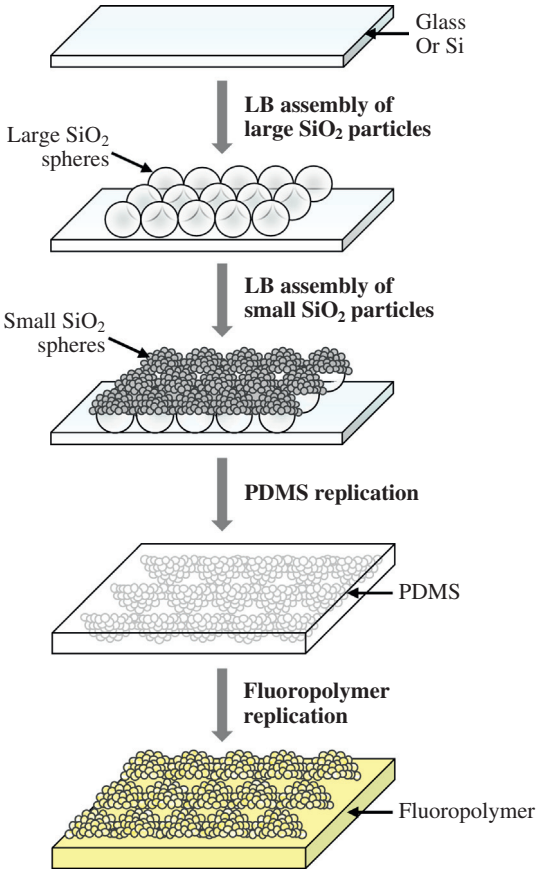

Fig. 1. Schematic illustration of the colloidal self-assembly and templating processes for fabricating superhydrophobic surface with hierarchical periodic micro-/nano-structures.

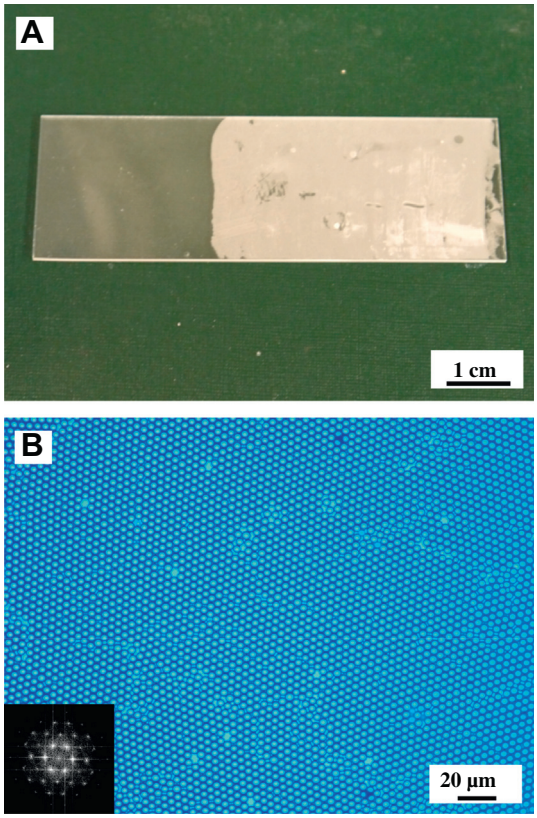

Fig. 2. (A) Photograph of a glass microslide (75 × 25 mm) covered with a LB-assembled colloidal monolayer of 4 μm silica spheres. (B) Optical microscope image of the sample in (A). Inset showing a Fourier transform of a lower-magnification optical microscope image.

quality of the close-packed monolayer colloidal crystal created by LB assembly. Although intrinsic defects such as point defects and grain boundaries are present, the hexagonally ordered single crystal domains extend over 100s of micrometers. In our LB assembly technology, the floating of large silica spheres at the air/water interface is critical for the subsequent assembly of these particles into monolayer colloidal crystals. As the density of silica (ρ_{silica} ~ 2.0 g/cm^3) is higher than that of water, the surface tension force must dominate the gravitational force to let the silica spheres float at the air/water interface. We can compare the importance of the gravitational force to the surface tension force by using the dimensionless Bond number (B_0) which is defined as [56]:

$$B_0 = \frac{\Delta\rho g L^2}{\sigma} \quad (1)$$

where $\Delta\rho$ is the density difference between silica and water, g is the gravitational acceleration, L is the characteristic length (here, is the radius of silica spheres), and σ is the surface tension of water (72.75 mN/m at 20 °C) [57]. For both 4 and 30 μm silica spheres, the calculated B_0 is much less than 1, indicating that surface tension dominates. The use of ethylene glycol as the solvent to disperse silica spheres is also critical for our LB assembly technique. The silica–ethylene glycol suspension first spreads over the water surface to form a thin floating layer. With the gradual dissolution of ethylene glycol in water, silica spheres can then be accumulated at the air/water interface. The capillary actions between neighboring silica particles finally organize the floating particles into close-packed monolayer colloidal crystals at the air/water interface [43,53].

The same LB technique is repeated to deposit monolayers of 300 nm silica microspheres on the above large sphere arrays. Fig. 3A–D shows typical top- and side-view SEM images at

different magnification levels of the resulting binary colloidal arrays consisting of 4 μm and 300 nm silica particles. The hexagonal ordering of small microspheres on the contoured surfaces of large spheres is clearly evident. The high flexibility of a thin water layer that is observed to carry the floating silica microspheres during the particle transfer process, as well as strong capillary action between the small microspheres contribute to the observed conformal coverage of the curved large spheres by the close-packed small particle monolayers.

Our LB assembly technique can be easily extended to fabricate binary colloidal arrays using spheres with a wide range of sizes. Fig. 4A–D shows typical top-view SEM images at different magnification levels for a binary silica array consisting of 30 μm and 300 nm particles. Both large and small spheres are arranged into hexagonally ordered, close-packed monolayer arrays. As the capillary force between neighboring spheres protruding out of the floating water film, which is the major driving force for the spontaneous crystallization of the colloidal monolayers, is proportional to the surface tension of water and the radius of the spheres [58], it is expected that the crystalline quality of colloidal arrays consisting of larger spheres could be better than that of smaller spheres. This is true for submicrometer-scale microspheres. Our experiments show that silica microspheres with diameter smaller than 100 nm are difficult to be assembled by the LB approach, while larger microspheres with diameter smaller than 1 μm are easy to be assembled into high-quality colloidal monolayers [47]. For even larger silica spheres, the slow crystallization kinetics retards the formation of large crystalline domains at the air/water interface. Gentle agitation, such as continuous tapping of the sidewall of the crystallizing dish, can significantly improve the quality of the resulting large sphere colloidal crystals.

The LB-assembled binary colloidal arrays can be directly used as superhydrophobic substrates after a simple surface modification process using various fluorosilanes. The fluorosilanes can form dense molecular monolayers on the surface of silica particles through the well-established silane coupling reactions [59]. Fig. 5 shows the profile of a water droplet on the binary colloidal array shown in Fig. 3 after surface modification using (tridecafluoro-1,1,2,2,-tetrahydrooctyl)-trichlorosilane. The substrate is superhydrophobic and the measured apparent water CA is ~153°. This CA value compares favorably to those obtained on binary particle arrays fabricated by various top-down and bottom-up approaches [20,30–34,46]. Compared with these previous techniques, one major advantage of the LB assembly approach is that both sides of the substrate can be simultaneously coated with the superhydrophobic binary particle arrays. However, the direct utilization of the self-assembled hierarchical particle arrays as superhydrophobic substrates suffers from several drawbacks. First, the durability of the fluorosilane molecules on silica particles, which play a critical role in achieving the final superhydrophobic surface state, is a major concern [60–62]. Second, the throughput of this bottom-up technique is low as the deposited binary colloidal arrays can only be used on a single substrate and cannot be reused on the other substrates. Third, the weak adhesion of the particle arrays on the substrate could significantly affect the environmental stability of the resulting coatings. Thermal annealing or chemical treatment of the coatings are generally performed to improved their mechanical properties [31,33].

To greatly improve the throughput and mechanical/chemical stability of the superhydrophobic substrates, we develop a simple templating technology to fabricate monolithic fluoropolymer coatings with hierarchical micro-/nano-structures. In this approach, the LB-assembled binary colloidal arrays are first used as structural templates to make flexible PDMS molds. Multiple copies of fluoropolymer superhydrophobic coatings can then be replicated on various substrates. The intrinsic low surface energy of fluoropolymers coupled with the hierarchical structure-induced dewetting facilitates the realization of superhydrophobic surface states even without any surface modification process. In this work, we synthesize a UV-curable perfluoroether acrylate – UV-T with the molecular structure shown in Scheme 1 by following the established synthetic procedures [51]. The absorption bands in the FTIR spectrum (not shown here) of the as-prepared monomers match with the reported vibrations [51,63]. The low-viscosity liquid monomers

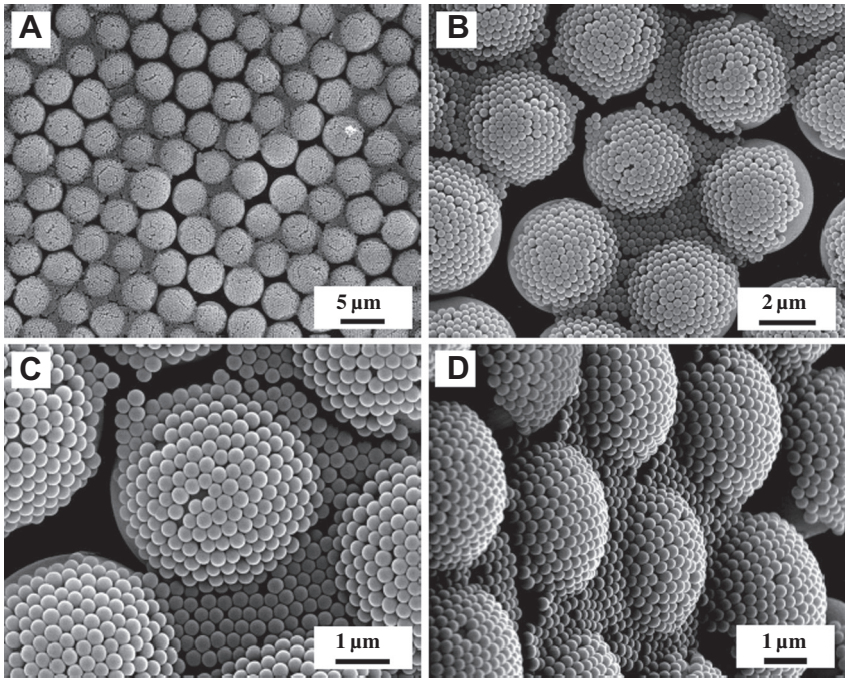

Fig. 3. (A–C) Typical top-view SEM images of a LB-assembled binary colloidal array consisting of 4 μm and 300 nm silica spheres. (D) Typical side-view SEM image of the same sample.

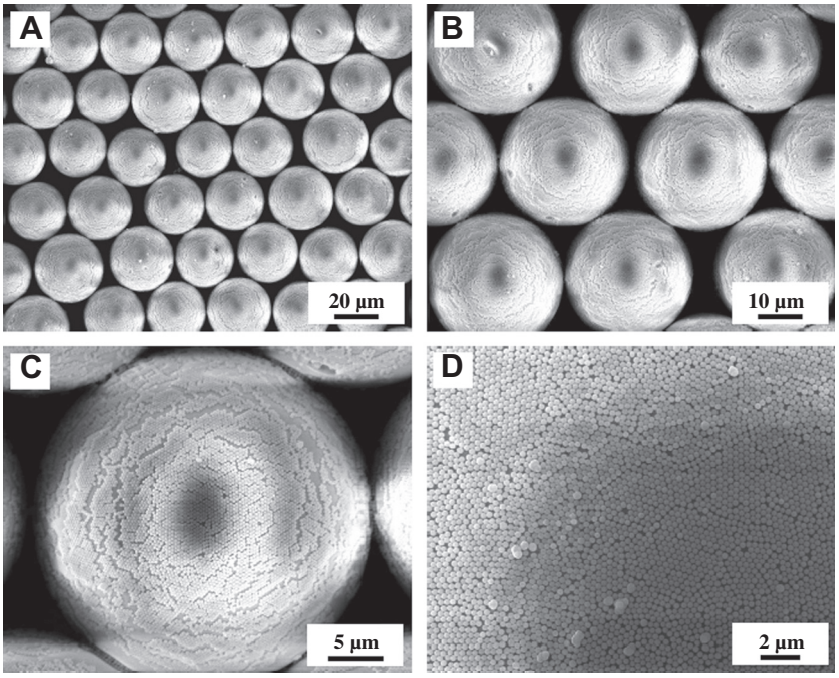

Fig. 4. Typical top-view SEM images at different magnification levels of a binary colloidal array consisting of 30 μm and 300 nm silica spheres.

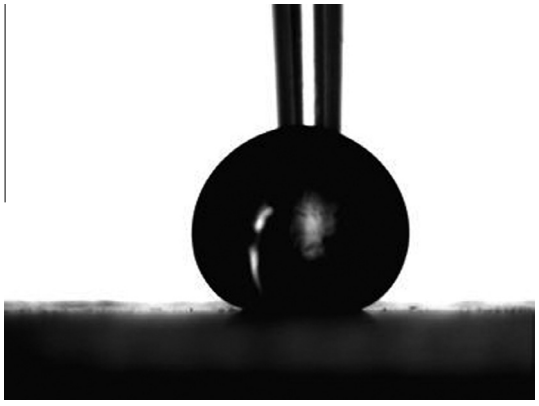

Fig. 5. Water drop profile on a fluorosilane-modified binary colloidal array consisting of 4 μm and 300 nm silica spheres.

UV-T:

$$R_1CH_2\text{-}Rf\text{-}CH_2R_1$$

$R_1 =$ $R_2CH_2CH(R_2)CH_2O-$
$R_2 =$ $CH_2{=}CHCO_2-$
$Rf =$ $-CF_2O(CF_2CF_2O)_m(CF_2O)_nCF_2-$

Scheme 1. Molecular structure of a UV-curable perfluoroether acrylate (UV-T) used for templating superhydrophobic fluoropolymer surfaces with hierarchical micro-/nano-structures.

enable easy replication, and the resulting polymer films are highly flexible due to the extremely low glass transition temperature (ca. −90 °C) of UV-T [51].

Fig. 6A shows a top-view SEM image of a PDMS mold just peeled off from the binary colloidal array consisting of 30 μm and 300 nm silica spheres as shown in Fig. 4. The low surface energy of PDMS ensures that no large silica particles are detached from the substrate, while only a very small amount of 300 nm microspheres is adhered on the surface of the PDMS mold. These

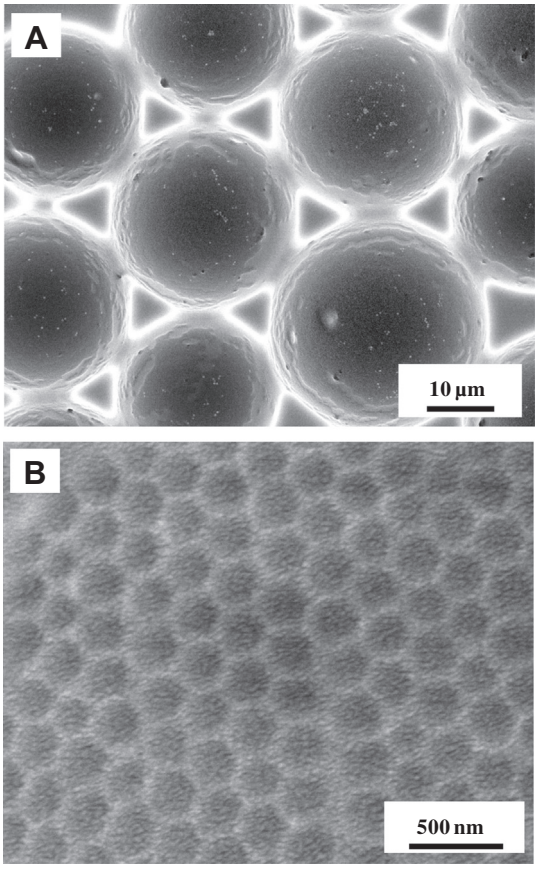

Fig. 6. (A) Typical top-view SEM image of a PDMS mold replicated from the binary colloidal array consisting of 30 μm and 300 nm silica spheres. (B) A higher-magnification SEM image.

small silica particles can be easily removed by dissolving in a hydrofluoric acid aqueous solution (2 vol%) for 2–3 min. The

average diameter of the large voids which are templated from the large silica spheres matches with the diameter of the large spheres, indicating that only the top hemispherical caps of the binary colloidal arrays are replicated into the final PDMS mold. This is caused by the high viscosity of the two-part PDMS precursors which prevents the full penetration of the precursors into the interstitials of the particle arrays. Similar hemispherical replication is observed for the small voids which are templated from 300 nm silica microspheres as revealed by the magnified SEM image in Fig. 6B. The preservation of the hexagonal ordering of the original 300 nm silica monolayer (see Fig. 4D) is clearly evident.

The PDMS mold with the replicated hierarchical void structure can finally be used as a second-generation template to make multiple copies of structured UV-T films by simple and rapid photopolymerization. The adhesion of UV-T on the substrates (e.g., glass or silicon) can be significantly improved by priming the substrates with 3-acryloxypropyl trichlorosilane [64]. Figs. 7A and B present SEM images of a templated UV-T array using the PDMS mold shown in Fig. 6. The replicated large and small hemispherical arrays keep the same hexagonal close-packed structure and the lattice spacing as the original binary colloidal array (Fig. 4).

Dynamic CA measurements are performed to evaluate the superhydrophobic performance of the templated UV-T arrays with hierarchical micro-/nano-structures. The static water drop profile in Fig. 8A shows that the apparent water CA on the hierarchical UV-T array is ~152°, indicating a superhydrophobic surface. By contrast, a flat UV-T film exhibits an intrinsic apparent water CA of ~107°. Previous studies show that the static water CA alone is insufficient for completely evaluating the dewetting properties of superhydrophobic substrates [65]. We therefore measure the advancing and receding CAs associated with the increase and

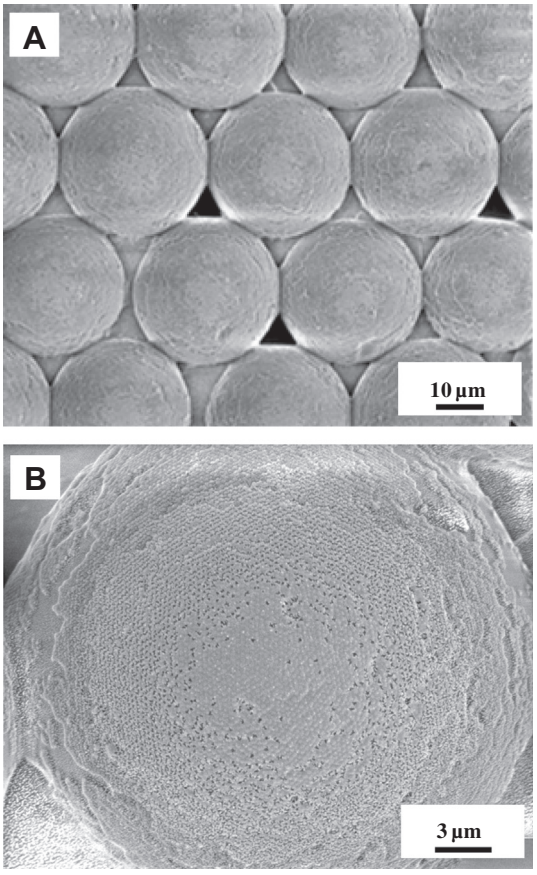

Fig. 7. (A) Typical top-view SEM image of a templated UV-T array with hierarchical periodic micro-/nano-structures. (B) A higher-magnification SEM image.

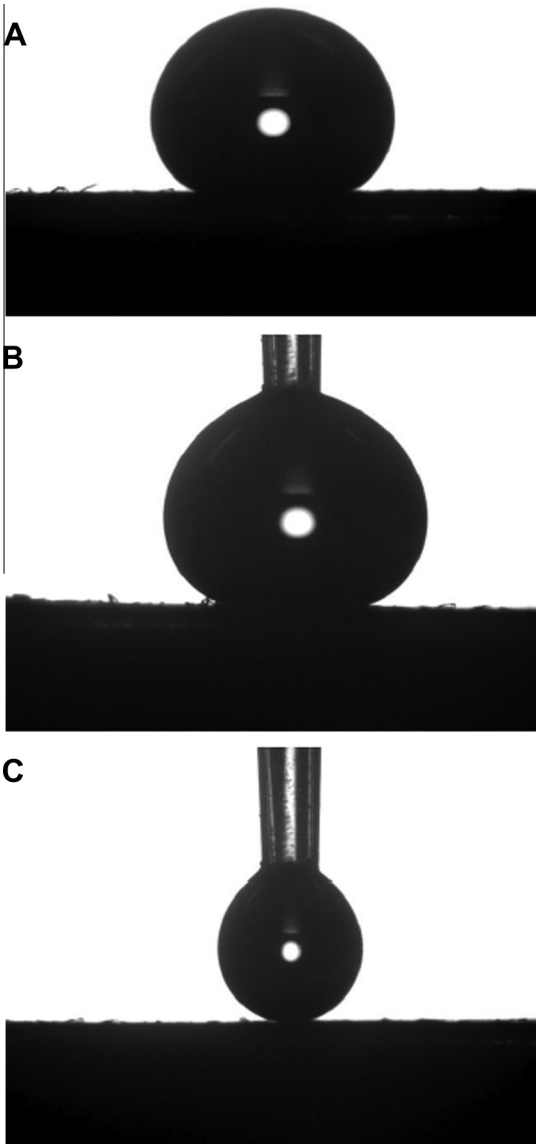

Fig. 8. Water drop profiles show (A) apparent water CA, (B) advancing water CA, and (C) receding water CA on a templated UV-T array with hierarchical periodic micro-/nano-structures.

decrease in droplet volumes using the same dynamic CA analyzer. Fig. 8B and C show the water drop profiles used to measure the advancing and receding CAs on the UV-T hierarchical array. The corresponding advancing and receding CAs are ~154° and ~150°, indicating a very small CA hysteresis, which is equally important as large CAs for superhydrophobic substrates in many relevant applications [66].

To gain better understanding of the dewetting behaviors exhibited by the templated fluoropolymer hierarchical arrays, we complement the experimental CA measurements with theoretical predictions using the well-established Cassie's model [49], which has been widely used for calculating water CAs on structured hydrophobic materials. In Cassie's model, the water droplet wets a composite surface consisting of both solid (UV-T in this case) and entrapped air. This incomplete wetting can be described by the Cassie equation:

$$\cos\theta' = f\cos\theta - (1-f) \tag{2}$$

where f is the fraction of the area of the fluoropolymer in direct contact with the water droplet. By inputting the experimental CA values into Eq. (2), we can estimate f to be ~0.165. This indicates

that a large fraction of air is trapped between the water droplet and the substrate, and water is prevented from entering into the large interstitials between the large UV-T hemispheres. The water droplet therefore sits presumably on the surfaces of the small fluoropolymer protrusions templated from small silica spheres. However, a UV-T control sample templated from a LB-assembled monolayer of 300 nm silica microspheres only exhibits an apparent water CA of ~126°, showing the importance of the hierarchical micro-/nano-structure in achieving superhydrophobic surface states.

4. Conclusions

In conclusion, we have developed a simple colloidal self-assembly technology for fabricating superhydrophobic coatings with hierarchical periodic micro-/nano-structures that mimic natural compound eyes of many insects. The LB assembly technology does not require sophisticated equipment (e.g., a LB trough) and is compatible with scalable roll-to-roll processing. It enables the spontaneous crystallization of silica particles with a wide range of sizes into hexagonally ordered, close-packed monolayer arrays on both flat and curved surfaces (e.g., contoured spherical surfaces). The surface-modified binary colloidal arrays and the templated fluoropolymer hierarchical arrays are all superhydrophobic. Theoretical calculations based on the Cassie's dewetting model predict that a large fraction of air is entrapped in the final superhydrophobic coatings with hierarchical structures. Besides providing a new approach in fabricating superhydrophobic surfaces, our simple bottom-up technology could pave a unique way in assembling biomimetic periodic hierarchical arrays with unprecedented optical properties for a wide spectrum of important technological applications ranging from artificial compound eyes [2,67] to broadband antireflection coatings [23].

Acknowledgments

Acknowledgments are made to the National Science Foundation (Grant Nos. CBET-0744879 and CMMI-1000686), the Donors of the American Chemical Society Petroleum Research Fund, the UF Research Opportunity Seed Fund, and National Science Council (Grant No. NSC 102-2218-E-005-005-MY2) for support of this research.

References

[1] D.G. Stavenga, S. Foletti, G. Palasantzas, K. Arikawa, Proc. R. Soc. B 273 (2006) 661.
[2] L.P. Lee, R. Szema, Science 310 (2005) 1148.
[3] T.L. Sun, L. Feng, X.F. Gao, L. Jiang, Acc. Chem. Res. 38 (2005) 644.
[4] X.J. Feng, L. Jiang, Adv. Mater. 18 (2006) 3063.
[5] P. Roach, N.J. Shirtcliffe, M.I. Newton, Soft Matter 4 (2008) 224.
[6] A. Tuteja, W. Choi, M.L. Ma, J.M. Mabry, S.A. Mazzella, G.C. Rutledge, G.H. McKinley, R.E. Cohen, Science 318 (2007) 1618.
[7] K.S. Liu, Y. Tian, L. Jiang, Prog. Mater. Sci. 58 (2013) 503.
[8] K.S. Liu, L. Jiang, Annu. Rev. Mater. Res. 42 (2012) 231.
[9] A.R. Parker, C.R. Lawrence, Nature 414 (2001) 33.
[10] Y.M. Zheng, H. Bai, Z.B. Huang, X.L. Tian, F.Q. Nie, Y. Zhao, J. Zhai, L. Jiang, Nature 463 (2010) 640.
[11] Z.Z. Gu, H. Uetsuka, K. Takahashi, R. Nakajima, H. Onishi, A. Fujishima, O. Sato, Angew. Chem. Int. Ed. 42 (2003) 894.
[12] O. Sato, S. Kubo, Z.Z. Gu, Acc. Chem. Res. 42 (2009) 1.
[13] S.H. Kim, S.Y. Lee, S.M. Yang, G.R. Yi, NPG Asia Mater. 3 (2011) 25.
[14] A.K. Geim, S.V. Dubonos, I.V. Grigorieva, K.S. Novoselov, A.A. Zhukov, S.Y. Shapoval, Nat. Mater. 2 (2003) 461.
[15] A. Mahdavi, L. Ferreira, C. Sundback, J.W. Nichol, E.P. Chan, D.J.D. Carter, C.J. Bettinger, S. Patanavanich, L. Chignozha, E. Ben-Joseph, A. Galakatos, H. Pryor, I. Pomerantseva, P.T. Masiakos, W. Faquin, A. Zumbuehl, S. Hong, J. Borenstein, J. Vacanti, R. Langer, J.M. Karp, Proc. Natl. Acad. Sci. USA 105 (2008) 2307.
[16] I.A. Aksay, M. Trau, S. Manne, I. Honma, N. Yao, L. Zhou, P. Fenter, P.M. Eisenberger, S.M. Gruner, Science 273 (1996) 892.
[17] L.J. Bonderer, A.R. Studart, L.J. Gauckler, Science 319 (2008) 1069.
[18] F. Barthelat, Philos. Trans. R. Soc. A 365 (2007) 2907.
[19] C. Ortiz, M.C. Boyce, Science 319 (2008) 1053.
[20] X.F. Gao, X. Yan, X. Yao, L. Xu, K. Zhang, J.H. Zhang, B. Yang, L. Jiang, Adv. Mater. 19 (2007) 2213.
[21] P.B. Clapham, M.C. Hutley, Nature 244 (1973) 281.
[22] W.L. Min, B. Jiang, P. Jiang, Adv. Mater. 20 (2008) 3914.
[23] H.B. Xu, N. Lu, G. Shi, D.P. Qi, B.J. Yang, H.B. Li, W.Q. Xu, L.F. Chi, Langmuir 27 (2011) 4963.
[24] J. Zhu, Z.F. Yu, G.F. Burkhard, C.M. Hsu, S.T. Connor, Y.Q. Xu, Q. Wang, M. McGehee, S.H. Fan, Y. Cui, Nano Lett. 9 (2009) 279.
[25] E. Bittoun, A. Marmur, Langmuir 28 (2012) 13933.
[26] F. Bottiglione, G. Carbone, Langmuir 29 (2013) 599.
[27] Y.H. Xue, S.G. Chu, P.Y. Lv, H.L. Duan, Langmuir 28 (2012) 9440.
[28] Y.Y. Yan, N. Gao, W. Barthlott, Adv. Colloid Interface Sci. 169 (2011) 80.
[29] C.C. Yang, V. Castelvetro, S. Bianchi, M. Alderighi, Y.M. Zhang, J. Colloid Interface Sci. 378 (2012) 210.
[30] Y. Zhao, M. Li, Q.H. Lu, Z.Y. Shi, Langmuir 24 (2008) 12651.
[31] W. Ming, D. Wu, R. van Benthem, G. de With, Nano Lett. 5 (2005) 2298.
[32] H.J. Tsai, Y.L. Lee, Langmuir 23 (2007) 12687.
[33] G. Zhang, D.Y. Wang, Z.Z. Gu, H. Mohwald, Langmuir 21 (2005) 9143.
[34] Y.H. Xiu, L.B. Zhu, D.W. Hess, C.P. Wong, Langmuir 22 (2006) 9676.
[35] Y. Huang, J.M. Zhou, B. Su, L. Shi, J.X. Wang, S.R. Chen, L.B. Wang, J. Zi, Y.L. Song, L. Jiang, J. Am. Chem. Soc. 134 (2012) 17053.
[36] J.Y. Shiu, C.W. Kuo, P.L. Chen, C.Y. Mou, Chem. Mater. 16 (2004) 561.
[37] X.T. Zhang, O. Sato, M. Taguchi, Y. Einaga, T. Murakami, A. Fujishima, Chem. Mater. 17 (2005) 696.
[38] A.M. Brozell, M.A. Muha, A. Abed-Amoli, D. Bricarello, A.N. Parikh, Nano Lett. 7 (2007) 3822.
[39] S.H. Kim, S.Y. Lee, S.M. Yang, Angew. Chem. Int. Ed. 49 (2010) 2535.
[40] C.T. Hsieh, F.L. Wu, W.Y. Chen, Mater. Chem. Phys. 121 (2010) 14.
[41] Q. Chen, S.C. Bae, S. Granick, Nature 469 (2011) 381.
[42] J. Yan, M. Bloom, S.C. Bae, E. Luijten, S. Granick, Nature 491 (2012) 578.
[43] B.G. Prevo, O.D. Velev, Langmuir 20 (2004) 2099.
[44] P. Jiang, J.F. Bertone, K.S. Hwang, V.L. Colvin, Chem. Mater. 11 (1999) 2132.
[45] A. Blanco, E. Chomski, S. Grabtchak, M. Ibisate, S. John, S.W. Leonard, C. Lopez, F. Meseguer, H. Miguez, J.P. Mondia, G.A. Ozin, O. Toader, H.M. van Driel, Nature 405 (2000) 437.
[46] H.T. Yang, P. Jiang, J. Colloid Interface Sci. 352 (2010) 558.
[47] K. Askar, B.M. Phillips, X. Dou, J. Lopez, C. Smith, B. Jiang, P. Jiang, Opt. Lett. 37 (2012) 4380.
[48] B.M. Phillips, P. Jiang, B. Jiang, Appl. Phys. Lett. 99 (2011) 191103.
[49] A.B.D. Cassie, S. Baxter, Trans. Faraday Soc. 40 (1944) 546.
[50] W. Stöber, A. Fink, E. Bohn, J. Colloid Interface Sci. 26 (1968) 62.
[51] R. Blomquist, L. Eldada, M.J. McFarland, C. Poga, L.W. Shacklette, Proc. SPIE 3799 (1999) 266.
[52] L.W. Shacklette, R. Blomquist, J.M. Deng, P.M. Ferm, M. Maxfield, J. Mato, H. Zou, Adv. Funct. Mater. 13 (2003) 453.
[53] N.D. Denkov, O.D. Velev, P.A. Kralchevsky, I.B. Ivanov, H. Yoshimura, K. Nagayama, Nature 361 (1993) 26.
[54] E.P. Plueddemann, Silane Coupling Agents, second ed., Plenum Press, New York, NY, 1991.
[55] Y. Coffinier, S. Janel, A. Addad, R. Blossey, L. Gengembre, E. Payen, R. Boukherroub, Langmuir 23 (2007) 1608.
[56] F.P. Incropera, D.P. DeWitt, T.L. Bergman, A.S. Lavine, Introduction to Heat Transfer, fifth ed., John Wiley & Sons, Hoboken, NJ, 2007.
[57] D.R. Lide, H.P.R. Frederikse, CRC Handbook of Chemistry and Physics, 76th ed., CRC Press, Boca Raton, FL, 1995.
[58] P.A. Kralchevsky, K. Nagayama, Langmuir 10 (1994) 23.
[59] C. Gellermann, W. Storch, H. Wolter, J. Sol–Gel Sci. Technol. 8 (1997) 173.
[60] L. Boinovich, A.M. Emelyanenko, A.S. Pashinin, ACS Appl. Mater. Interface 2 (2010) 1754.
[61] Z. Cui, L. Yin, Q.J. Wang, J.F. Ding, Q.M. Chen, J. Colloid Interface Sci. 337 (2009) 531.
[62] X.T. Zhu, Z.Z. Zhang, J. Yang, X.H. Xu, X.H. Men, X.Y. Zhou, J. Colloid Interface Sci. 380 (2012) 182.
[63] C.H. Sun, A. Gonzalez, N.C. Linn, P. Jiang, B. Jiang, Appl. Phys. Lett. 92 (2008) 051107.
[64] P. Jiang, M.J. McFarland, J. Am. Chem. Soc. 126 (2004) 13778.
[65] M. Miwa, A. Nakajima, A. Fujishima, K. Hashimoto, T. Watanabe, Langmuir 16 (2000) 5754.
[66] W. Choi, A. Tuteja, J.M. Mabry, R.E. Cohen, G.H. McKinley, J. Colloid Interface Sci. 339 (2009) 208.
[67] K.H. Jeong, J. Kim, L.P. Lee, Science 312 (2006) 557.